JOURNAL OF GUIDANCE, CONTROL, AND DYNAMICS
Vol. 18, No. 2, March–April 1995

Autonomous Rendezvous Using Artificial Potential Function Guidance

Ismael Lopez* and Colin R. McInnes†
University of Glasgow, Glasgow G12 8QQ, Scotland, United Kingdom

A novel methodology has been developed for the guidance and control of a maneuvering chase vehicle undergoing terminal rendezvous in the presence of path constraints and multiple obstructions. The method hinges on defining a suitable scalar function which represents an artificial potential field describing the locality of the target vehicle. Using a set of bounded impulses the chase vehicle is guided by the local topology of this potential function. Obstructions and path constraints are introduced by superimposing regions of high potential around these regions. Exact, analytical expressions are then obtained for the required control impulse magnitude, direction and switching times using the second method of Lyapunov. These control impulses ensure that the potential function monotonically decreases so that convergence of the chaser to the target is ensured analytically, without violating the path constraints. Since the components of the potential and control impulses may be represented analytically, the method appears suitable for autonomous, real-time control of complex maneuvers with a minimum of onboard computational power.

Introduction

RENDEZVOUS problems have become of increasing importance in recent years due to space station applications. Relatively simple analytical solutions which provide the impulses required for achieving rendezvous after a specified interval of time have long been established. These are the well-known Clohessy–Wiltshire rendezvous solutions.[1] Subsequent studies have investigated minimum propellant rendezvous maneuvers using optimal control theory.[2–5] More recently expert systems have been developed for automated terminal rendezvous guidance.[6] However, such systems require complex software and place demands on onboard computational power. Similarly, human path planning has been considered for space station operations. In general, such methodologies result in feasible solutions but place an extra burden on crew work load.[7]

Most studies assume that the chase vehicle may access any region of the configuration space. However, many scenarios of future orbital operations involve operations in the proximity of large space structures, such as the proposed international space station. In most cases, accidental contact of a vehicle with another structure is hazardous. Consequently, one of the essential requirements for operations near large space structures is the ability to maneuver in proximity to them without collision. Moreover, such scenarios may include additional constraints such as obstructions which are fixed or moving with respect to the target. Such obstructions may be another spacecraft, station-keeping near the target, or a nonphysical volume, such as an antenna radiation beam. An acceptable transfer in such an environment is one which ensures rendezvous but which does not intersect the obstructions. Additionally, to reduce the operational cost and complexity of such systems, it is desirable that the guidance is simple but entirely autonomous.

The problem of path-constrained maneuvering was initially introduced by Stern and Fowler.[8] It was demonstrated that only a small fraction of unbroken transfer paths between arbitrary points on representative structural shapes successfully completed point-to-point transfers, without first colliding with the structure.[9,10] However, this method involves numerically intensive techniques, allows only the calculation of the statistical likelihood of a particular maneuver being successful, and does not provide real-time guidance information.

In this study the guidance information is provided by superimposing an artificial potential function on the system state space.[11] The local topology of this potential generates analytic guidance commands, obtained using the second method of Lyapunov. These guidance commands ensure the convergence of the chaser to the target by guiding the chaser along a path of steepest descent. The method provides analytical expressions for the required control impulse magnitude, direction, and switching times.

The motivation for this approach has been to develop an analytically based method which ensures convergence to the target without collisions. This safety critical criterion has been taken to be paramount. As such the method is not optimal, although the propellant costs for terminal rendezvous are, in general, not large. The potential function method has already been successfully applied to proximity maneuvering of low-thrust vehicles.[11] The potential function method itself has its origins in robotics,[12,13] although terrestrial robots have, in principle, access to systems with large computational power. For this reason robotic application have centred on numerically generated potentials.[14]

Obstructions are handled by superimposing regions of high potential about the volume of state space to be avoided. By manipulating the local topology of the obstruction potentials, different geometries of obstructions may be considered. The path may then be shaped in any desired manner by manipulating the global topology of the potential function. Therefore, the vehicle may complete a collision-free rendezvous maneuver between any two points in state space using analytic guidance commands. Since the guidance is entirely analytical, it is believed that this methodology may be suitable for the real-time, autonomous guidance of terminal rendezvous maneuvers, using a minimum of onboard computational power.

Proximity Equations

The dynamical equations describing the relative motion between the target and chase vehicle will now be formulated. Figure 1 shows the position vectors of the target $\boldsymbol{r}_T$ on an arbitrary circular orbit and chaser $\boldsymbol{r}$ with respect to the geocentric frame. The relative position of the chaser with respect to the target is defined by the vector $\boldsymbol{L}$ resolved into a local Cartesian frame x (r bar), y (v bar) and z (out of plane). It will be assumed that there are no non-gravitational perturbations other than the chaser control impulses. The vector equation of motion of the chase vehicle in a reference frame rotating with the target is then given by

$$\ddot{\boldsymbol{r}} + 2\boldsymbol{w} \times \dot{\boldsymbol{r}} + \boldsymbol{w} \times (\boldsymbol{w} \times \boldsymbol{r}) = -\nabla\phi \qquad (1)$$

Received Oct. 18, 1993; revision received July 12, 1994; accepted for publication July 12, 1994.

*Research Assistant, on leave of absence from Universidad Politecnica de Madrid.

†Lecturer, Department of Aerospace Engineering.

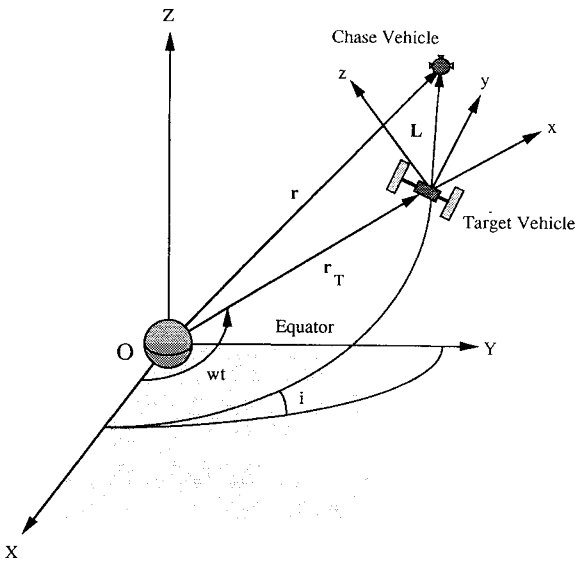

Fig. 1 Rendezvous coordinate system.

where w is the target orbital angular velocity vector and ϕ the local two-body gravitational potential.

Assuming that the target-to-chaser distance is much smaller than the orbital radius of the target satellite, Eq. (1) may be linearized by transforming to target fixed coordinates $L = r - r_T$, viz.,

$$\ddot{L} + 2w \times \dot{L} + w \times (w \times L) = -\left\{\frac{\partial}{\partial r}\nabla\phi\right\}L + \mathcal{O}(L^2) \quad (2)$$

Nondimensionalizing the local target fixed coordinates such that $\xi = (x/r_T), \eta = (y/r_T), \zeta = (z/r_T)$ and changing the independent variable to azimuthal angle $\nu = wt$ it is found that

$$\xi'' - 2\eta' - 3\xi = 0 \quad (3a)$$

$$\eta'' + 2\xi' = 0 \quad (3b)$$

$$\zeta'' + \zeta = 0 \quad (3c)$$

where the prime denotes differentiation with respect to the azimuthal angle. These are the familiar Clohessy–Wiltshire equations which may now be used to develop the potential function guidance methodology.

Potential Function Guidance

The second method of Lyapunov will now be used to generate guidance commands and to ensure convergence of the chaser to the target. A suitable scalar potential function $V(x)$ is now chosen with $V(\mathbf{0}) = \mathbf{0}$ such that

$$V(x) > 0, \qquad \forall x \neq \mathbf{0} \quad (4a)$$

$$V(x) \to \infty, \qquad \text{as} \qquad \|x\| \to \infty \quad (4b)$$

$$V'(x) < 0, \qquad \forall x \neq \mathbf{0} \quad (4c)$$

With these conditions the state-space origin is a globally attractive point, with all state-space paths converging toward it.[15] The state vector x to be considered in the subsequent analysis will contain only position variables $x = (\xi, \eta, \zeta)$, so that in principle Lyapunov's theorem will only ensure convergence in position and not in velocity. However, it will be demonstrated that velocity convergence is, in fact, ensured through the controls chosen.

Conditions (4a) and (4b) may be satisfied by the choice of a suitable positive definite scalar potential function $V(x)$. The third condition (4c) will be imposed by choosing a suitable set of impulsive controls. To this end, the total derivative of the potential $V(x)$ may be written as

$$\frac{\mathrm{d}V}{\mathrm{d}\nu} = \frac{\partial V}{\partial \nu} + \{\nabla_x V(x)\}^T x' \quad (5)$$

However, in this study the potential will be time independent and so independent of ν. When $V' < 0$ the motion of the chase vehicle is freely propagated but, when V' vanishes, a control impulse will be provided such that the condition $V' < 0$ is again satisfied. If Eq. (5) is now solved for a vector of control impulses such that V' is globally negative definite, then a control law is obtained which renders the closed-loop system globally and asymptotically stable. Therefore, the vehicle will be brought to the origin from any point in state space, within the linear regime.

In the subsequent analysis the local topology of the potential function will be used to shape the path of the maneuvering vehicle. Therefore, to obtain a vector of control impulses which is linear in the state-space coordinates and to allow easy modifications of the potential shape, a quadratic form will be used as the potential function, viz.,

$$V(x) = x^T P x \quad (6)$$

Since the chosen state vector is a function of position only, the control impulses will be provided such that the chaser velocity $x'(\nu)$ immediately after an impulse $\Delta x'(\nu)$ is directly opposite to the local potential gradient, viz.,

$$x'(\nu) + \Delta x'(\nu) = -k\nabla_x V(x) \quad (7)$$

where k is a positive gain. This condition then defines a proper control[16] at the impulse application and ensures that the chase vehicle motion immediately following an impulse is tangent to the potential gradient. This is an essential condition for the subsequent analysis of path-constrained maneuvering.

Unconstrained Rendezvous

To illustrate the use of potential function guidance, a simple unconstrained rendezvous maneuver will be considered. The following positive definite matrix will be used with Eq. (6) to give an ellipsoidal projection of the potential in the configuration space:

$$P = \begin{Bmatrix} p_1 & 0 & 0 \\ 0 & p_2 & 0 \\ 0 & 0 & p_3 \end{Bmatrix} \quad (8)$$

such that the potential function becomes $V(x) = p_1\xi^2 + p_2\eta^2 + p_3\zeta^2$. The potential ellipsoid is always aligned with the target fixed coordinate axes. However, a congruent transformation of Eq. (6) may be used to rotate the ellipsoid.

Using Eq. (7) the control impulse $\Delta x'(\nu) = (\Delta\xi', \Delta\eta', \Delta\zeta')$ may be calculated such that the chaser velocity vector after a control impulse is directly opposite to the potential gradient. This condition may be written compactly as

$$\frac{\xi' + \Delta\xi'}{p_1\xi} = \frac{\eta' + \Delta\eta'}{p_2\eta} = \frac{\zeta' + \Delta\zeta'}{p_3\zeta} = -k \quad (9)$$

These three conditions then define the control impulse magnitude and direction whereas Eq. (5) defines the switching times. The rate of descent of the potential immediately after an impulse is then found to be

$$V'(x) = -2k\left\{(p_1\xi)^2 + (p_2\eta)^2 + (p_3\zeta)^2\right\} \quad (10)$$

Since the rate of descent of the potential is now negative definite, global asymptotic convergence is ensured, but only in position since the state vector is a function of position only. However, the chosen control impulses also ensure convergence in velocity space, as the vehicle velocity after an impulse is bounded by a monotonically decreasing quantity. From Eq. (9) it can be seen that after an impulse the chaser velocity is given by

$$\|x'\| = k\sqrt{(p_1\xi)^2 + (p_2\eta)^2 + (p_3\zeta)^2} \to 0, \qquad \|x\| \to 0 \quad (11)$$

so that rendezvous is ensured.

Figure 2 shows the path of the chase vehicle to the target using the controls defined by Eq. (9), with the vehicle guided along the path of steepest descent of the potential. The vehicle state is propagated

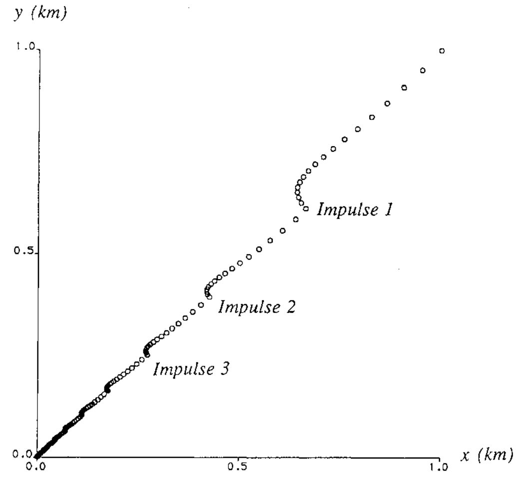

Fig. 2 Unconstrained rendezvous.

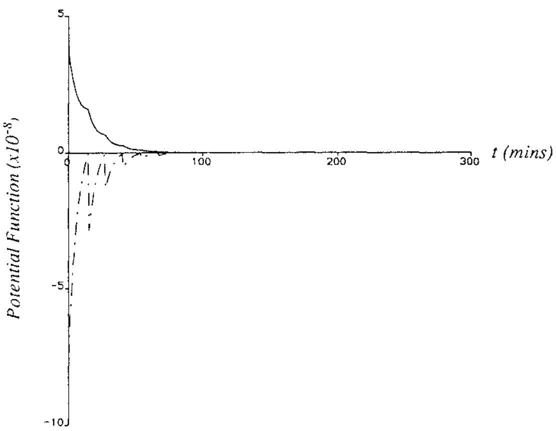

Fig. 3 Potential (nondimensional), ——, and rate of descent of potential, - - - -.

using the standard linear Clohessy-Wiltshire equations. It is found that 14 impulses and a Δv of 2.77 ms^{-1} is required to bring the chaser to within 1 m of the target. A total Δv of 2.51 ms^{-1} is required for an optimal two-impulse transfer. The duration of the potential guided maneuver is 210 min. However, since the approach is asymptotic, most of this time is required to close the final meters of the rendezvous. Since the guidance is autonomous the duration of the maneuver has not been considered as a critical parameter. It is envisaged, however, that a rescaling of the potential in the terminal phase would greatly reduce the total number of impulses and maneuver duration if required.

It can be seen that the chaser trajectory close to the target is almost rectilinear since the elapsed time between successive impulses becomes small as the chaser closes to the target. Figure 3 shows the nondimensional potential function and rate of descent of the potential function with time. As can be seen, the potential is monotonically decreasing since its total time derivative is negative definite. Each discontinuity in the rate of descent of the potential represents a control impulse being applied to the vehicle.

Obstruction Avoidance

The methodology developed in the previous section will now be extended to include obstructions which are fixed with respect to the target.[11] The previous methodology required convergence of all trajectories to the target. Now, not only will convergence be considered, but it will be required that the trajectories do not cross the obstruction surfaces. To enforce this requirement the obstructions will be isolated by regions of high artificial potential, Fig. 4. Gaussian functions will be used to represent the obstructions, so that the controls obtained are bounded and no singularities are introduced in

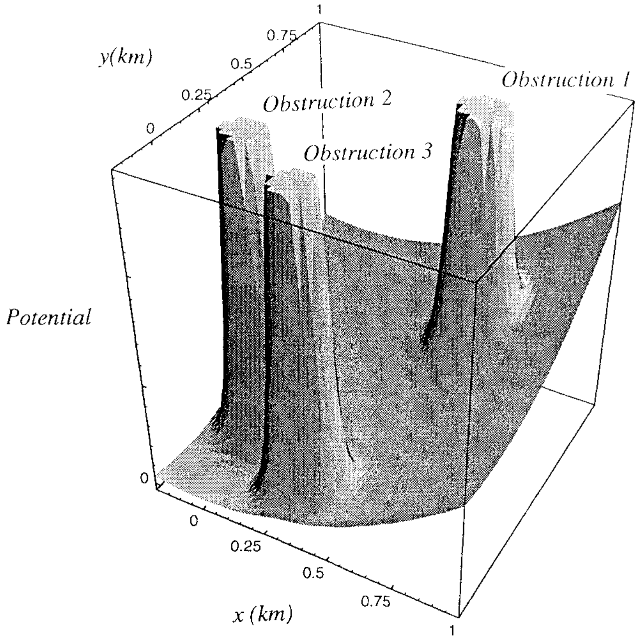

Fig. 4 Quadratic potential function with obstructions.

the potential function. The shape of the obstruction potential may be easily modified through the width and skewness of the Gaussian to generate a maximal surface entirely enclosing the obstruction. The obstruction potential function will then defined to be of the form

$$\Psi(\boldsymbol{x}, \tilde{\boldsymbol{x}}) = \Psi_1 \exp\{-\sigma^{-1}(\boldsymbol{x} - \tilde{\boldsymbol{x}})^T M(\boldsymbol{x} - \tilde{\boldsymbol{x}})\} \qquad (12)$$

where the obstruction is located at state space position $\tilde{\boldsymbol{x}}$. The parameters σ and Ψ_1 are assignable, defining the width and height of the obstruction potential. They are chosen such that the absolute value of the potential at the obstruction surface is equal to the potential at the initial vehicle position. Therefore, since V is monotonically decreasing, the chase vehicle trajectory can never cross an obstruction surface and so cannot collide with the obstructions.

The matrix $\boldsymbol{M}$ defines the shape of the potential to represent the boundary of the obstruction. For example, if the boundary is spherical it may be described with the matrix $\boldsymbol{M} = \text{diag}(1, 1, 1)$. The augmented potential is now defined by a superposition of the quadratic form of Eq. (6) and the obstruction potentials as

$$V(\boldsymbol{x}, \tilde{\boldsymbol{x}}_k) = \boldsymbol{x}^T \boldsymbol{P} \boldsymbol{x} + \sum_{k=1}^{K} \Psi_k(\boldsymbol{x}, \tilde{\boldsymbol{x}}_k) \qquad (13)$$

However, using this form of obstruction potential several difficulties are introduced. Conditions (3a) and (3b) of the Lyapunov's theorem are still valid, however, the potential may no longer have a unique minimum at $\boldsymbol{x} = \boldsymbol{0}$ as additional local minima may be introduced with the obstruction potentials. However, for simple configurations it may be shown that these local minima are unstable saddle points, so that there remains a unique, globally attractive point. Furthermore, due to the superimposed obstruction potentials, the location of the global minimum is no longer exactly at the origin of the target fixed coordinates. However, due to the rapid truncation of the obstruction potentials, this displacement of the global minimum is negligible. In fact, for the terminal guidance strategy discussed later, this difficulty will not arise.

Rendezvous with Multiple Obstructions

A path-constrained rendezvous will now be considered with multiple obstructions. Again, an impulse will be applied to the vehicle when V' vanishes such that the chase vehicle velocity vector immediately after an impulse is directly opposite to the local potential gradient. Using the matrix $\boldsymbol{P}$ defined by Eq. (8) and $\boldsymbol{M}$ as

$$\boldsymbol{M} = \begin{Bmatrix} m_1 & 0 & 0 \\ 0 & m_2 & 0 \\ 0 & 0 & m_3 \end{Bmatrix} \tag{14}$$

the required controls $\Delta \boldsymbol{x}'(\nu) = (\Delta\xi', \Delta\eta', \Delta\zeta')$ are now calculated from Eq. (7) using the following expression

$$\frac{\xi' + \Delta\xi'}{p_1\xi - \lambda_1} = \frac{\eta' + \Delta\eta'}{p_2\eta - \lambda_2} = \frac{\zeta' + \Delta\zeta'}{p_3\zeta - \lambda_3} = -k \tag{15a}$$

where

$$\lambda_1 = \sum_{k=1}^{K} m_1 \frac{\Psi_k}{\sigma_k}(\xi - \tilde{\xi}_k)\Lambda_k \tag{15b}$$

$$\lambda_2 = \sum_{k=1}^{K} m_2 \frac{\Psi_k}{\sigma_k}(\eta - \tilde{\eta}_k)\Lambda_k \tag{15c}$$

$$\lambda_3 = \sum_{k=1}^{K} m_3 \frac{\Psi_k}{\sigma_k}(\zeta - \tilde{\zeta}_k)\Lambda_k \tag{15d}$$

$$\Lambda_k = \exp\Big\{ -\sigma_k^{-1}\big\{m_1(\xi - \tilde{\xi}_k)^2 + m_2(\eta - \tilde{\eta}_k)^2 + m_3(\zeta - \tilde{\zeta}_k)^2\big\}\Big\} \tag{15e}$$

and k is again a positive gain.

Velocity space convergence is again ensured since the magnitude of the chaser velocity after the impulse is always bounded by

$$\|\boldsymbol{x}'\| = k\sqrt{(p_1\xi - \lambda_1)^2 + (p_2\eta - \lambda_2)^2 + (p_3\zeta - \lambda_3)^2} \tag{16}$$

It can be seen that in principle the chaser has a small (typically $< 10^{-3}$ ms^{-1}) residual relative velocity of $(\lambda_1^2 + \lambda_2^2 + \lambda_3^2)^{\frac{1}{2}}$ at the origin due to the obstruction potentials. However, this problem does not arise as the terminal guidance strategy will ensure an exact rendezvous. The rate of descent of the potential after the impulse is then found to be

$$V'(\boldsymbol{x}) = -2k\big\{(p_1\xi - \lambda_1)^2 + (p_2\eta - \lambda_2)^2 + (p_3\zeta - \lambda_3)^2\big\} \tag{17}$$

Since V' is negative definite, global convergence is again ensured.

Figure 5 illustrates the vehicle path with three fixed obstructions. From the initial state the chaser is guided to the target using a set of bounded, decreasing impulses, which ensure not only convergence but also obstruction avoidance. To bring the chaser to within 1 m of the origin of the target fixed coordinates it is found that 94 impulses and a total Δv of 42 ms^{-1} is required. This increase in the Δv requirement over the unconstrained case is representative of the highly constrained path of the chase vehicle. The large number of impulses is largely due to the final, almost rectilinear approach to the target. Most of the impulses are required during this slow terminal phase. Such maneuvering requires repeated impulses to generate a quasicontinuous control. The total duration of the maneuver is 225 min. Again, much of this time is required for closing the final meters of the approach.

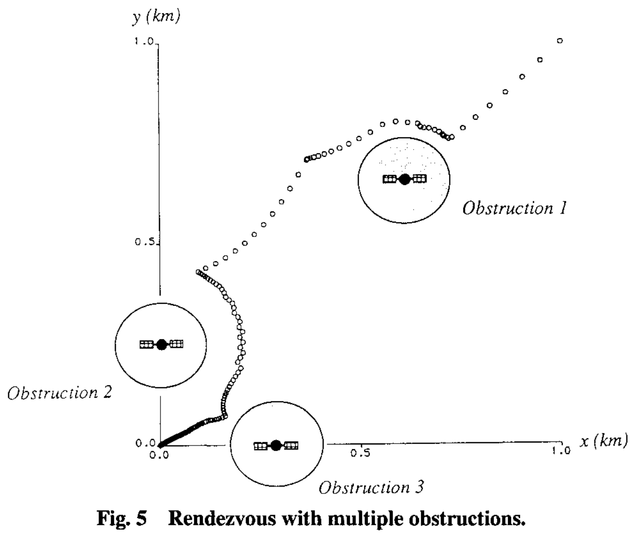

Fig. 5 Rendezvous with multiple obstructions.

Terminal Rendezvous Guidance

In the previous section the problem of convergence in position and velocity in the presence of obstructions was discussed. However, no constraint was imposed on the chase vehicle at the final approach to the target. The final approach of a real rendezvous is constrained to be performed along the target docking axis. Therefore, target obstruction constraints must be developed, to take into account these path constraints at the final approach. These constraints will be imposed by superimposing a high-potential surface around the target to guide the chase vehicle to the docking axis from any initial approach direction.

The shape of the boundary chosen is similar to a cardioid but is composed of three semiellipses, as shown in Fig. 6. Semiellipses I and II provide the constraint that the final approach has to be performed along the positive y axis. Since semiellipses I and II are tangent to the y axis at the origin, the final meters of the approach are performed essentially along the docking axis. Semiellipse III provides the constraint that the chaser must fly around the target to reach the positive y axis. A three-dimensional constraint surface is obtained by rotating the target constraint with respect to the y axis.

The parameters b, a_1, and b_1 defined in Fig. 6 must be chosen to avoid generating local minima at points A_1 and A_2. It is easy to demonstrate that the following conditions must hold to ensure that a local minimum is not formed at these points between the target constraint potential and the quadratic potential

$$b > 2\sqrt{(p_1/p_2)}a_1 \tag{18a}$$

$$b > 2\sqrt{(p_3/p_2)}a_1 \tag{18b}$$

$$p_2 < 2\left\{\frac{a_1}{b_1}\right\}^2 p_1 \tag{18c}$$

$$p_2 < 2\left\{\frac{a_1}{b_1}\right\}^2 p_3 \tag{18d}$$

The distance d_1 from the origin to the target constraint boundary may be obtained in polar coordinates as

$$d_1 = \frac{2a_1b_1^2\cos\theta}{b_1^2\cos^2\theta + a_1^2\sin^2\theta}, \qquad \theta \in [0, \pi/2) \tag{19a}$$

$$d_1 = \frac{2a_1b_1^2\cos\theta}{b_1^2\cos^2\theta + a_1^2\sin^2\theta}, \qquad \theta \in [\pi/2, \pi) \tag{19b}$$

$$d_1 = \frac{2a_1b_1}{\sqrt{b^2\cos^2\theta + 4a_1^2\sin^2\theta}}, \qquad \theta \in [\pi, 2\pi) \tag{19c}$$

The controls are then generated in two regions with conditions $r > r_1$ or $r < r_1$ where $r_1 = \max(d_1)$, $\theta \in [0, 2\pi)$, and $r = (\xi^2 + \eta^2 + \zeta^2)^{\frac{1}{2}}$.

1) If $r > r_1$ then the quadratic potential will be augmented with the obstruction potentials, as defined by Eq. (13).

2) If $r \leq r_1$ the potential will contain the target constraint only. The obstruction potentials are then not included to avoid disturbing the global minimum from the origin.

Case 2 will then be considered with the condition $r \geq d_1$. When $r = d_1$, so that the chase vehicle is on the target constraint, an impulse must be applied, such that the rate of descent of the potential function is again negative definite. The direction of the impulse will be chosen such that the chase vehicle velocity vector after the impulse bisects between the tangent vector to the boundary at this

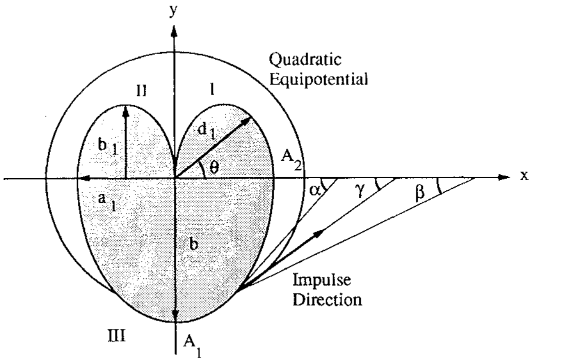

Fig. 6 Target constraint potential.

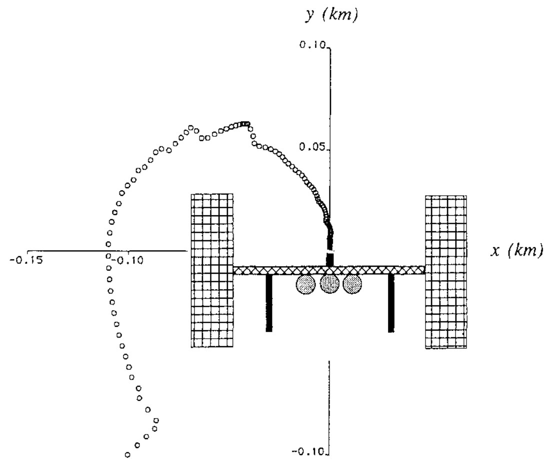

Fig. 7 Terminal approach with target constraints.

point and the tangent vector to the quadratic equipotential curve at the same point. The direction of the vehicle velocity vector is then defined by the angle $\gamma = (\alpha + \beta)/2$, Fig. 6.

Using this control the impulse magnitude is such that the chase vehicle velocity after an impulse application is again bounded by the quantity

$$\|x'\| = k\sqrt{(p_1\xi)^2 + (p_2\eta)^2 + (p_3\zeta)^2} \to 0, \qquad \|x\| \to 0 \quad (20)$$

This equation then bounds the vehicle velocity just after the impulse when $d_1 \leq r \leq r_1$.

Figure 7 illustrates a typical chase vehicle trajectory during terminal approach. The vehicle is guided autonomously to the origin of the target fixed coordinates by a set of bounded, decreasing impulses, such that the vehicle is successfully driven to the docking axis nonetheless avoiding the obstruction generated by the target itself. The last few meters of the final approach are performed following the docking axis. This distance can be modified with the parameter b_1 and adjusted to the desired length. It can be seen that the chase vehicle tightly follows the potential until it finally hops along the boundary and onto the docking axis. An additional Δv of 8 ms^{-1} is required for this maneuver.

Conclusions

The methodology developed in this study has been demonstrated to be successful in that path-constrained rendezvous may be ensured analytically, from any state-space position. The chase vehicle is guided autonomously by a set of bounded impulse controls from any initial state to rendezvous with the target. The impulse magnitude and direction are obtained analytically, derived from an artificial potential function by applying the second method of Lyapunov. The burn times are defined as the instant when the rate of descent of the potential vanishes.

Obstructions may be handled by superimposing regions of high potential about the volume of state space to be avoided. Moreover, various geometries of obstructions may be considered by manipulating the potential shape. The vehicle may, therefore, complete a collision-free rendezvous maneuver, using exact analytical controls. The path and behavior of the vehicle when considering obstructions is rather complex, however, the method is able to control such complex behavior using compact analytic guidance commands.

A degree of optimization has been achieved in that the chaser velocity vector after the impulse is directly opposite to the potential gradient. With this method, the number of impulses necessary to accomplish the rendezvous is reduced and, therefore, the global propellant use is also reduced. However, since the goal of this study has been to develop an analytically based, collision-free method, explicit fuel optimization has not been guaranteed or, indeed, obtained. To do so would require significantly more complex numerical methods which defeat the initial goals of the study. These goals have traded fuel optimization for a globally convergent method which guarantees safe, collision-free rendezvous in the presence of obstructions. Since the vehicle is guided autonomously using exact, analytic guidance commands, a minimum of onboard computational power is required so that the methodology appears suitable for onboard, real-time implementation.

Acknowledgments

Funding for I. Lopez was provided from the European ERASMUS program and the Universidad Politecnica de Madrid.

References

[1]Clohessy, W. H., and Wilshire, R. S., "Terminal Guidance System for Satellite Rendezvous," *Journal of Aerospace Science*, Vol. 27, No. 9, 1960, pp. 653–674.

[2]Porcelli, G., and Daniel, T., "Fuel Time-Optimal Rendezvous by Nonlinear Programming," *Acta Astronautica*, Vol. 16, No. 3, 1964, pp. 167–172.

[3]Prussing, J. E., "Optimal Two- and Three-Impulse Fixed-Time Rendezvous in the Vicinity of a Circular Orbit," *AIAA Journal*, Vol. 8, 1970, pp. 1221–1228.

[4]Carter, T., "Fuel-Optimal Rendezvous Near a Point in General Keplerian Orbit," *Journal of Guidance, Control, and Dynamics*, Vol. 10, No. 6, 1987, pp. 567–573.

[5]Van der Ha, J. C., "Analytical Solutions for Fuel-Optimal Rendezvous by Finite-Thrust Arcs," 42nd International Astronautical Congress, IAF-91-363, Montreal, Canada, Oct. 1991.

[6]Olszewski, O. W., "Automated Terminal Guidance for a Shuttle Rendezvous to Space Station Freedom," *Proceedings of the AIAA Guidance, Navigation, and Control Conference*, AIAA, Washington DC, 1990, pp. 337–387.

[7]Grunwald, A. J., and Ellis, S. R., "Visual Display Aid for Orbital Maneuvering: Design Considerations," *Journal of Guidance, Control, and Dynamics*, Vol. 16, No. 1, 1993, pp. 139–144.

[8]Stern, S. A., and Fowler, W. T., "Path Constrained Rendezvous Near Large Space Structures," *Journal of Spacecraft and Rockets*, Vol. 22, 1985, pp. 548–553.

[9]Soileau, K. M., and Stern, S. A., "Path-Constrained Rendezvous: Necessary and Sufficient Conditions," *Journal of Spacecraft and Rockets*, Vol. 23, 1986, pp. 492–498.

[10]Soileau, K. M., "Defining Optimal Point-To-Point Transfer Surfaces for Orbital Path-Constrained Rendezvous," Proceedings of the AAS/NASA International Symposium on Spaceflight Dynamics, AAS 89-161, NASA Goddard Spaceflight Center, April 1989.

[11]McInnes, C. R., "Autonomous Proximity Maneuvering Using Artificial Potential Functions," *European Space Agency Journal*, Vol. 17, No. 2, 1993, pp. 159–169.

[12]Khatib, O., "Real-Time Obstacle Avoidance for Manipulators and Mobile Robots," *International Journal of Robotics Research*, Vol. 5, No. 1, 1986, pp. 90–99.

[13]Rimon, E., and Koditschek, D. E., "Exact Robot Navigation Using Artificial Potential Functions," *Transactions on Robotics and Automation*, Vol. 8, No. 5, 1992, pp. 501–518.

[14]Sato, K., "Deadlock-free Motion Planning Using the Laplace Potential Field," *Advanced Robotics*, Vol. 7, No. 5, 1993, pp. 449–461.

[15]Csaki, F., *Modern Control Theories: Nonlinear, Optimal and Adaptive Systems*, Akademiai Kiado, Budapest, Hungary 1972, pp. 441–500.

[16]Grantham, W. J., and Chingcuanco, A. O., "Lyapunov Steepest Descent Control of Constrained Linear Systems," *Transactions on Automatic Control*, Vol. AC-29, No. 8, 1984, pp. 740–743.